Orbit Uncertainty Propagation around Non-Spherical Bodies
Using the Dromo Formulation

By Javier HERNANDO-AYUSO,[1] and Claudio BOMBARDELLI[2]

[1]*Department of Aeronautics and Astronautics, The University of Tokyo, Tokyo, Japan*
[2]*Space Dynamics Groups, Technical University of Madrid, Spain*

In this paper, a numerical scheme for the calculation of the State Transition Matrix (STM) based on the Dromo formulation is presented. Dromo is a special perturbation method that offers important advantages both for the numerical propagation and for the analytical analysis of perturbed orbital motion. The obtained STM incorporates the perturbing effects of the primary body oblateness and the gravitational influence of third bodies. We apply this STM to the problem of orbit uncertainty propagation. The proposed method is found to be less complex than non-linear methods, both from the mathematical and the computational point of view, and overcomes fundamental limitations of linear methods based on Cartesian coordinates. The method is especially accurate for low eccentricity orbits (e < 0.1), and outperforms in any case a linear propagation performed using Cartesian coordinates.

Nomenclature

C	:	covariance matrix
G	:	Dromo state vector gradient matrix
I	:	identity matrix
J	:	Jacobian matrix
P, Q, R	:	rotation matrices
Φ	:	State Transition Matrix
f	:	perturbing acceleration vector
g	:	Dromo state vector time-derivative
q, q	:	Dromo state vector, Dromo element
r	:	position vector
v	:	velocity vector
a	:	semi-major axis
e	:	eccentricity
h	:	orbit angular momentum
i	:	orbit inclination
k	:	J2 perturbation coefficient
N	:	number of perturbing bodies
n	:	mean motion
$\tilde{n}$	:	inverse of the unit of time
$\tilde{r}$	:	unit of length
s	:	transversal velocity
u	:	radial velocity
v_x, v_y, v_z	:	velocity vector components
x, y, z	:	position vector components
α_2	:	J2 perturbation proportionality constant
β	:	fictitious-time drift
μ	:	gravitational parameter of the primary
ν	:	true anomaly
τ	:	time
σ	:	fictitious time / standard deviation
Ω	:	right ascension of the ascending node
ω	:	argument of periapsis
$\mathcal{I}$	:	inertial frame
$\mathcal{R}$	:	local vertical local horizontal frame
$\mathcal{P}$	:	intermediate frame

Subscripts

0	:	initial epoch
r	:	radial direction
θ	:	transversal direction
h	:	out-of-plane direction
j	:	index of perturbing body
$0, s, c, s2, c2$	:	linear, sin or cos of a multiple of σ

1. Introduction

The capability of efficiently assess how state uncertainties propagate is crucial in many space science and technology applications. In general, any kind of state uncertainty can be propagated using a Monte-Carlo (MC) method with a full nonlinear model. The main limitation of this approach is computation time: the need to propagate individual points of a sufficiently well discretized initial state for a long period of time is typically very expensive. This is why MC methods are employed in limited cases or for validating other more computationally efficient methods.

The need to obtain a computationally efficient scheme to propagate uncertainties without missing key features of the orbit dynamics has motivated the search of alternative solutions. On one hand, the limitations of linear covariance propagation in Cartesian elements, unable to follow the complex and highly non-linear uncertainty evolution, have been mitigated by the use of classical or equinoctial orbital elements. [1] The use of curvilinear coordinates to propagate the orbit uncertainty has also been proven to be advantageous. [2] Other authors have employed higher-order Taylor series expansion in Cartesian elements [3] or Gaussian mixture sampling techniques [4] to better track the non-linear evolution of the uncertainty domain.

Following a similar approach to Ref. 1, the authors have very recently explored the use of another set of elements for uncertainty propagation: the so called "Dromo elements" derived from a relatively recent orbital motion formulation proposed by Pelaez et al. in 2007 [5] and considerably improved in subse-

quent works by Urrutxua et al. [6], Baú et al. in 2013, [7] 2014 [8] and 2015 [9]. Using this formulation, the *linear* propagation of the uncertainty of Near Earth Asteroids (NEAs) subject to N-body perturbation [10] was presented recently and shown to drastically improve its Cartesian counterpart. The excellent results obtained for the NEAs case motivated the investigation of an orbit uncertainty propagation scheme applied to Earth-bound orbits.

As a first step, we perform a derivation of a generalized state transition matrix (STM) in Dromo elements accounting for the main geopotential term. and third-body perturbations (Sun and Moon). Once the time evolution of the STM is obtained the covariance matrix propagation can be carried out analytically bringing a dramatic improvement compared to Monte-Carlo methods.

The key question regarding the range of validity of the proposed uncertainty propagation scheme, depending on the size of the initial uncertainty region and the propagation time interval considered, is addressed by an extensive campaign of numerical simulations.

Results show that the evolution of the uncertainty of satellites considering the typical orbit determination errors and time propagation of Earth orbiting satellites can be represented quite well with the proposed method. As expected, the Cartesian propagation of the covariance rapidly fails to represent the error distribution when propagated away from the initial epoch.

2. Dromo formulation

Let us consider a particle of mass m orbiting around a primary at initial radial position r_0 measured from the center of the primary and angular position ν_0 measured from the initial eccentricity vector in the initial orbital plane (and hence corresponding to the initial true anomaly). Let us employ, from now on and unless specified, the Earth equatorial radius $\tilde{r}$ as unit of distance, $1/\tilde{n}$ as the unit of time (τ) where $\tilde{n}$ is the angular rate of a *circular* orbit with radius equal to the reference radius $\tilde{r}$:

$$\tilde{n} = \sqrt{\frac{\mu}{\tilde{r}^3}}, \tag{1}$$

with μ indicating the gravitational parameter of the primary.

The Dromo formulation is characterized by the use of a fictitious time σ as independent variable as given by the Sundmann transformation:

$$\frac{d\tau}{d\sigma} = \frac{r^2}{h}, \tag{2}$$

where h denotes the angular momentum of the particle and r its radius. The physical interpretation of the variable σ is found by integrating the previous equation after conveniently setting $\sigma_0 = \nu_0$, to obtain:

$$\sigma = \nu + \beta, \tag{3}$$

which underlines that the variation of the fictitious time is related to the variation of the osculating true anomaly by the addition of an *angular drift* β due to the action of orbital perturbations.

Seven generalized orbital elements $q_1, ..., q_7$, whose definition in relation to the classical orbital elements is given in the following.

The first three generalized orbital elements are defined as:

$$q_1 = \frac{e}{h}\cos\beta, \tag{4}$$

$$q_2 = \frac{e}{h}\sin\beta, \tag{5}$$

$$q_3 = \frac{1}{h}. \tag{6}$$

It is useful to derive the expression of the initial dimensionless angular momentum:

$$h_0 = \frac{\dot{\nu}_0 r_0^2}{\tilde{n}\tilde{r}^2} = \sqrt{\frac{(1 + e_0\cos\nu_0)\, r_0}{\tilde{r}}}, \tag{7}$$

and the initial value of the above generalized orbital elements:

$$q_{10} = \frac{e_0\,\sqrt{\tilde{r}}}{\sqrt{r_0\,(1 + e_0\cos\nu_0)}}, \tag{8}$$

$$q_{20} = 0, \tag{9}$$

$$q_{30} = \frac{\sqrt{\tilde{r}}}{\sqrt{r_0\,(1 + e_0\cos\nu_0)}}. \tag{10}$$

The four remaining generalized orbital elements are the Euler-Rodrigues parameters characterizing the rotation, associated to matrix $\boldsymbol{P}$, bringing an *intermediate frame* $\mathcal{P}$ (having two of its axes constantly lying in the instantaneous orbital plane of the particle) to overlap with a reference inertial frame ($\mathcal{I}$). In the classical Dromo formulation [5] the adopted intermediate frame was chosen in such a way to coincide with the (LVLH) orbital frame $\mathcal{R}$ at $\tau = 0$. Here we choose $\mathcal{P}$ in such a way that it coincides with the perifocal frame at $\tau = 0$ as done in Ref. 6).

$$\boldsymbol{P} = \begin{bmatrix} 1 - 2\left(q_5^2 + q_6^2\right) & 2\left(q_4q_5 - q_6q_7\right) & 2\left(q_4q_6 + q_5q_7\right) \\ 2\left(q_4q_5 + q_6q_7\right) & 1 - 2\left(q_4^2 + q_6^2\right) & 2\left(q_5q_6 - q_4q_7\right) \\ 2\left(q_4q_6 - q_5q_7\right) & 2\left(q_5q_6 + q_4q_7\right) & 1 - 2\left(q_4^2 + q_5^2\right) \end{bmatrix}, \tag{11}$$

An additional rotation matrix $\boldsymbol{Q}$ brings the orbital frame $\mathcal{R}$ attached to the particle to overlap with the intermediate frame $\mathcal{P}$ through a rotation of $-\sigma$ around the common z axis:

$$\boldsymbol{Q} = \begin{bmatrix} \cos\sigma & -\sin\sigma & 0 \\ \sin\sigma & \cos\sigma & 0 \\ 0 & 0 & 1 \end{bmatrix}. \tag{12}$$

Finally, the rotation from the $\mathcal{I}$ to the $\mathcal{R}$ frame is associated to the matrix:

$$\boldsymbol{R} = \boldsymbol{P}\boldsymbol{Q} \tag{13}$$

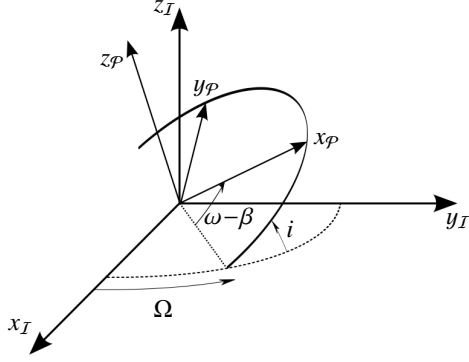The Euler Rodrigues parameters can be related to the classical orbital elements as:

$$q_4 = \sin\frac{i}{2}\cos\frac{\Omega - \omega + \beta}{2}, \tag{14}$$

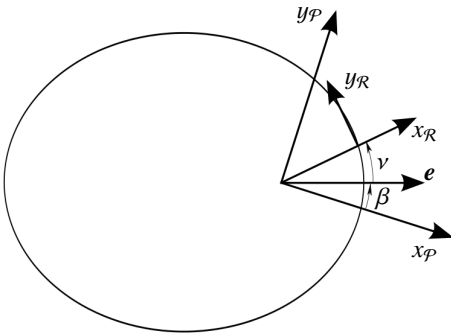$$q_5 = \sin\frac{i}{2}\sin\frac{\Omega - \omega + \beta}{2}, \tag{15}$$

$$q_6 = \cos\frac{i}{2}\sin\frac{\Omega + \omega - \beta}{2}, \tag{16}$$

$$q_7 = \cos\frac{i}{2}\cos\frac{\Omega + \omega - \beta}{2}. \tag{17}$$

The rotations between the references frames $\mathcal{I}$, $\mathcal{P}$ and $\mathcal{R}$ are shown in Fig. 1.

(a) Inertial ($\mathcal{I}$) and intermediate ($\mathcal{P}$) frames.

(b) Intermediate ($\mathcal{P}$) and LVLH ($\mathcal{R}$) frames.

Fig. 1.   Reference systems.

Other useful expressions are provided to obtain the classical orbital elements from the generalized Dromo elements as:

$$a = \frac{1}{q_3^2 - q_1^2 - q_2^2}, \tag{18}$$

$$e = \frac{1}{q_3} \sqrt{q_1^2 + q_2^2}, \tag{19}$$

$$i = \cos^{-1}\left(1 - 2\left(q_4^2 + q_5^2\right)\right), \tag{20}$$

$$\Omega = \operatorname{atan2}(q_5, q_4) + \operatorname{atan2}(q_6, q_7), \tag{21}$$

$$\omega = \operatorname{atan2}(q_2, q_1) + \operatorname{atan2}(q_6, q_7) - \operatorname{atan2}(q_5, q_4). \tag{22}$$

$$\nu = \sigma - \operatorname{atan2}(q_2, q_1), \tag{23}$$

Additional very useful formulas relate the Cartesian inertial position $\boldsymbol{r}$ and velocity $\boldsymbol{v}$ of the particle to the generalized orbital elements. They can be written in compact matrix form as:

$$\boldsymbol{r} = \boldsymbol{R}\begin{pmatrix} r \\ 0 \\ 0 \end{pmatrix} = r\,\boldsymbol{P}\begin{pmatrix} \cos\sigma \\ \sin\sigma \\ 0 \end{pmatrix}, \tag{24}$$

$$\boldsymbol{v} = \boldsymbol{R}\begin{pmatrix} u \\ s \\ 0 \end{pmatrix} = \boldsymbol{P}\begin{pmatrix} -q_2 - q_3\sin\sigma \\ q_1 + q_3\cos\sigma \\ 0 \end{pmatrix}, \tag{25}$$

where

$$s = q_3 + q_1\cos\sigma + q_2\sin\sigma \tag{26}$$

$$u = -\frac{\partial s}{\partial\sigma} = q_1\sin\sigma - q_2\cos\sigma \tag{27}$$

represents the transversal and radial components of the particle velocity, respectively. The orbit radius can be computed as:

$$r = \frac{1}{q_3 s}. \tag{28}$$

Finally, the evolution in time of the generalized orbital elements under the effect of the radial (f_r), transversal (f_θ), and out-of-plane (f_h) components of the dimensionless acceleration is governed by the differential equations:

$$\frac{\mathrm{d}}{\mathrm{d}\sigma}\begin{pmatrix} q_1 \\ q_2 \\ q_3 \end{pmatrix} = \frac{1}{q_3 s^3}\begin{bmatrix} s\sin\sigma & (s+q_3)\cos\sigma \\ -s\cos\sigma & (s+q_3)\sin\sigma \\ 0 & -q_3 \end{bmatrix}\begin{pmatrix} f_r \\ f_\theta \end{pmatrix}, \tag{29}$$

$$\frac{\mathrm{d}}{\mathrm{d}\sigma}\begin{pmatrix} q_4 \\ q_5 \\ q_6 \\ q_7 \end{pmatrix} = \frac{f_h}{2q_3 s^3}\begin{bmatrix} 0 & 0 & -\sin\sigma & \cos\sigma \\ 0 & 0 & \cos\sigma & \sin\sigma \\ \sin\sigma & -\cos\sigma & 0 & 0 \\ -\cos\sigma & -\sin\sigma & 0 & 0 \end{bmatrix}\begin{pmatrix} q_4 \\ q_5 \\ q_6 \\ q_7 \end{pmatrix}, \tag{30}$$

to be accompanied by the equation governing the evolution of the fictitious time:

$$\frac{\mathrm{d}\tau}{\mathrm{d}\sigma} = \frac{1}{q_3 s^2}. \tag{31}$$

After introducing the state vector $\boldsymbol{q} = (q_1, q_2, .., q_7, \sigma)^\top$ and the perturbing acceleration vector $\boldsymbol{f} = (f_r, f_\theta, f_h)^\top$, the preceding equations can be written in compact form with time as independent variable as:

$$\frac{\mathrm{d}\boldsymbol{q}}{\mathrm{d}\tau} = \boldsymbol{g}(\boldsymbol{q}, \boldsymbol{f}(\boldsymbol{q})). \tag{32}$$

where

$$g_1 = \frac{\mathrm{d}q_1}{\mathrm{d}\tau} = \frac{f_\theta}{s}(s+q_3)\cos\sigma + f_r\sin\sigma, \tag{33a}$$

$$g_2 = \frac{\mathrm{d}q_2}{\mathrm{d}\tau} = \frac{f_\theta}{s}(s+q_3)\sin\sigma - f_r\cos\sigma, \tag{33b}$$

$$g_3 = \frac{\mathrm{d}q_3}{\mathrm{d}\tau} = -f_\theta\frac{q_3}{s}, \tag{33c}$$

$$g_4 = \frac{\mathrm{d}q_4}{\mathrm{d}\tau} = \frac{f_h}{2s}(q_7\cos\sigma - q_6\sin\sigma), \tag{33d}$$

$$g_5 = \frac{\mathrm{d}q_5}{\mathrm{d}\tau} = \frac{f_h}{2s}(q_6\cos\sigma + q_7\sin\sigma), \tag{33e}$$

$$g_6 = \frac{\mathrm{d}q_6}{\mathrm{d}\tau} = -\frac{f_h}{2s}(q_5\cos\sigma - q_4\sin\sigma), \tag{33f}$$

$$g_7 = \frac{\mathrm{d}q_7}{\mathrm{d}\tau} = -\frac{f_h}{2s}(q_4\cos\sigma + q_5\sin\sigma), \tag{33g}$$

$$g_8 = \frac{\mathrm{d}\sigma}{\mathrm{d}\tau} = q_3 s^2. \tag{33h}$$

Here we highlight that the time-evolution of σ has no explicit dependence on the perturbing acceleration. In contrast, the time-evolution of the true anomaly reads (See Ref. 11, p. 489)

$$\frac{\mathrm{d}\nu}{\mathrm{d}t} = \frac{h}{r^2} + \frac{1}{e\,h}\left(\frac{h^2}{\mu}\cos\nu f_r - \left(\frac{h^2}{\mu} + r\right)\sin\nu f_\theta\right) \tag{34}$$

which directly depends on the perturbing accelerations. By the use of Eq. (3), it is possible to prove that the terms proportional to the perturbing acceleration in Eq. (34) correspond to the time derivative of the fictitious-time drift β.

3. State Transition Matrix

We can construct a State Transition Matrix (STM) in Dromo elements [10] . This constitutes a first approximation to the relative motion of a point mass moving in the vicinity of a reference orbit, q_{ref}. The evolution of the STM in Dromo elements is governed by

$$\frac{d\boldsymbol{\Phi}(\tau, \tau_0)}{d\tau} = \boldsymbol{G}(\tau)\, \boldsymbol{\Phi}(\tau, \tau_0) \tag{35}$$

which is to be integrated together with Eq. (33). The initial conditions are $\boldsymbol{\Phi}(\tau_0, \tau_0) = \boldsymbol{I_8}$, the eight-dimensional identity matrix. $\boldsymbol{G}$, the gradient matrix, corresponds to the following total derivative evaluated on the reference orbit

$$\boldsymbol{G} = \frac{d\boldsymbol{g}}{d\boldsymbol{q}} = \frac{\partial \boldsymbol{g}}{\partial \boldsymbol{q}} + \frac{\partial \boldsymbol{g}}{\partial \boldsymbol{f}} \frac{\partial \boldsymbol{f}}{\partial \boldsymbol{q}} \tag{36}$$

where $\boldsymbol{f}$ must be expressed in the $\mathcal{R}$ reference system.

The first derivative in the right hand side must be calculated for constant $\boldsymbol{f}$:

$$\frac{\partial \boldsymbol{g}}{\partial \boldsymbol{q}} = \begin{bmatrix} -\frac{f_\theta q_3 \cos^2 \sigma}{s^2} & -\frac{f_\theta q_3 \cos \sigma \sin \sigma}{s^2} & f_\theta \frac{s-q_3}{s^2} \cos \sigma & 0 & 0 & 0 & 0 & \frac{\partial g_1}{\partial \sigma} \\ -\frac{f_\theta q_3 \cos \sigma \sin \sigma}{s^2} & -\frac{f_\theta q_3 \sin^2 \sigma}{s^2} & f_\theta \frac{s-q_3}{s^2} \sin \sigma & 0 & 0 & 0 & 0 & \frac{\partial g_2}{\partial \sigma} \\ \frac{f_\theta q_3 \cos \sigma}{s^2} & \frac{f_\theta q_3 \sin \sigma}{s^2} & -f_\theta \frac{s-q_3}{s^2} & 0 & 0 & 0 & 0 & -f_\theta \frac{u}{s} \frac{q_3}{s} \\ -\frac{g_4 \cos \sigma}{s} & -\frac{g_4 \sin \sigma}{s} & -\frac{g_4}{s} & 0 & 0 & -\frac{f_h \sin \sigma}{2s} & \frac{f_h \cos \sigma}{2s} & \frac{g_4 u - g_5 s}{s} \\ -\frac{g_5 \cos \sigma}{s} & -\frac{g_5 \sin \sigma}{s} & -\frac{g_5}{s} & 0 & 0 & \frac{f_h \cos \sigma}{2s} & \frac{f_h \sin \sigma}{2s} & \frac{g_5 u + g_4 s}{s} \\ -\frac{g_6 \cos \sigma}{s} & -\frac{g_6 \sin \sigma}{s} & -\frac{g_6}{s} & \frac{f_h \sin \sigma}{2s} & -\frac{f_h \cos \sigma}{2s} & 0 & 0 & \frac{g_6 u - g_7 s}{s} \\ -\frac{g_7 \cos \sigma}{s} & -\frac{g_7 \sin \sigma}{s} & -\frac{g_7}{s} & -\frac{f_h \cos \sigma}{2s} & -\frac{f_h \sin \sigma}{2s} & 0 & 0 & \frac{g_7 u + g_6 s}{s} \\ 2q_3 s \cos \sigma & 2q_3 s \sin \sigma & s^2 + 2q_3 s & 0 & 0 & 0 & 0 & -2q_3 s\, u \end{bmatrix}, \tag{37}$$

with

$$\frac{\partial g_1}{\partial \sigma} = f_r \cos \sigma + f_\theta \left(-\left(1 + \frac{q_3}{s}\right) \sin \sigma + \frac{u}{s} \frac{q_3}{s} \cos \sigma \right), \tag{38}$$

$$\frac{\partial g_2}{\partial \sigma} = f_r \sin \sigma + f_\theta \left(\left(1 + \frac{q_3}{s}\right) \cos \sigma + \frac{u}{s} \frac{q_3}{s} \sin \sigma \right) \tag{39}$$

The second term is calculated considering a constant Dromo state vector:

$$\frac{\partial \boldsymbol{g}}{\partial \boldsymbol{f}} = \begin{bmatrix} \sin \sigma & \left(1 + \frac{q_3}{s}\right) \cos \sigma & 0 \\ -\cos \sigma & \left(1 + \frac{q_3}{s}\right) \sin \sigma & 0 \\ 0 & -\frac{q_3}{s} & 0 \\ 0 & 0 & \frac{1}{2s}(q_7 \cos \sigma - q_6 \sin \sigma) \\ 0 & 0 & \frac{1}{2s}(q_6 \cos \sigma + q_7 \sin \sigma) \\ 0 & 0 & -\frac{1}{2s}(q_5 \cos \sigma - q_4 \sin \sigma) \\ 0 & 0 & -\frac{1}{2s}(q_4 \cos \sigma + q_5 \sin \sigma) \\ 0 & 0 & 0 \end{bmatrix}. \tag{40}$$

A close orbit $\boldsymbol{q}$ is linearly propagated via the STM as

$$\boldsymbol{q} = \boldsymbol{q}_{\text{ref}} + \boldsymbol{\Phi}(\tau, \tau_0)(\boldsymbol{q}(\tau_0) - \boldsymbol{q}_{\text{ref}}(\tau_0)). \tag{41}$$

Finally, the covariance matrix expressed in Dromo elements can be propagated using the STM as well

$$\boldsymbol{C}(t) = \boldsymbol{\Phi}(\tau, \tau_0)\, \boldsymbol{C}(\tau_0)\, \boldsymbol{\Phi}(\tau, \tau_0)^\top. \tag{42}$$

3.1. N-body perturbation

The N-body perturbing acceleration can be written as:

$$\boldsymbol{f} = -\sum_{j=2}^{N-1} \mu_j \frac{\boldsymbol{r} - \boldsymbol{r}_j}{\|\boldsymbol{r} - \boldsymbol{r}_j\|^3} - \sum_{j=2}^{N-1} \mu_j \frac{\boldsymbol{r}_j}{\|\boldsymbol{r}_j\|^3} \tag{43}$$

where $j = 1$ is the primary body already considered in the Dromo formulation and $j = N$ is the object whose orbit is being analyzed, with mass negligible with respect to the perturbing bodies. $\boldsymbol{r}_j$ and μ_j are the position vector and the gravitational parameter of the jth body respectively.

It is important to underline that in order to derive analytical expressions for the 3×8 Jacobian matrix $\frac{\partial \boldsymbol{f}}{\partial \boldsymbol{q}}$ the perturbing acceleration $\boldsymbol{f}$ has to be projected onto the $\mathcal{R}$ reference frame. The representation of the particle position vector with respect to such frame is straightforward:

$$\boldsymbol{r}^{\mathcal{R}} = \left(\frac{1}{q_3 s}, 0, 0 \right)^\top. \tag{44}$$

The position of the jth body only depends on time and can be obtained using JPL's DE ephemeris [12] or VSOP [13] (*Variations Séculaires des Orbites Planétaires*). This position is usually expressed as a vector $\boldsymbol{r}_j^{\mathcal{I}}$ with respect to the inertial frame and can be projected onto $\mathcal{R}$ as follows

$$\boldsymbol{r}_j^{\mathcal{R}} = \boldsymbol{R}^\top \boldsymbol{r}_j^{\mathcal{I}}. \tag{45}$$

The derivative of the force components in $\mathcal{R}$ can now be obtained as:

$$\frac{\partial \boldsymbol{f}}{\partial \boldsymbol{q}} = \frac{\partial \boldsymbol{f}}{\partial \boldsymbol{r}^{\mathcal{R}}} \frac{\partial \boldsymbol{r}^{\mathcal{R}}}{\partial \boldsymbol{q}} + \sum_{j=2}^{N-1} \frac{\partial \boldsymbol{f}}{\partial \boldsymbol{r}_j^{\mathcal{R}}} \frac{\partial \boldsymbol{r}_j^{\mathcal{R}}}{\partial \boldsymbol{q}} \tag{46}$$

Reordering the terms in the summation, we obtain

$$\frac{\partial f}{\partial q} = -\sum_{j=2}^{N-1} \mu_j \left(\left(\frac{I_3}{\left\| r^{\mathcal{R}} - r_j^{\mathcal{R}} \right\|^3} - 3\frac{\left(r^{\mathcal{R}} - r_j^{\mathcal{R}}\right)\left(r^{\mathcal{R}} - r_j^{\mathcal{R}}\right)^\top}{\left\| r^{\mathcal{R}} - r_j^{\mathcal{R}} \right\|^5} \right) \left(\frac{\partial r^{\mathcal{R}}}{\partial q} - \frac{\partial r_j^{\mathcal{R}}}{\partial q} \right) + \left(\frac{I_3}{\left\| r_j^{\mathcal{R}} \right\|^3} - 3\frac{r_j^{\mathcal{R}} r_j^{\mathcal{R}\top}}{\left\| r_j^{\mathcal{R}} \right\|^5} \right) \frac{\partial r_j^{\mathcal{R}}}{\partial q} \right) \tag{47}$$

where I_3 is the 3-dimensional identity matrix, $y\,y^\top$ represents the outer product of the vector $y \in \mathbb{R}^3$ with itself which results in a 3-dimensional matrix, and

$$\frac{\partial r^{\mathcal{R}}}{\partial q} = \begin{bmatrix} -\frac{\cos\sigma}{q_3 s^2} & -\frac{\sin\sigma}{q_3 s^2} & -\frac{s+q_3}{q_3^2 s^2} & 0 & 0 & 0 & 0 & \frac{u}{q_3 s^2} \\ 0 & 0 & 0 & 0 & 0 & 0 & 0 & 0 \\ 0 & 0 & 0 & 0 & 0 & 0 & 0 & 0 \end{bmatrix}, \tag{48}$$

$$\frac{\partial r_j^{\mathcal{R}}}{\partial q} = \begin{bmatrix} 0 & 0 & 0 & | & \cdots & | & | \\ 0 & 0 & 0 & Q^\top \frac{\partial P^\top}{\partial q_4} R r_j^{\mathcal{R}} & \cdots & Q^\top \frac{\partial P^\top}{\partial q_7} R r_j^{\mathcal{R}} & \frac{\partial Q^\top}{\partial \sigma} Q r_j^{\mathcal{R}} \\ 0 & 0 & 0 & | & \cdots & | & | \end{bmatrix}, \tag{49}$$

with

$$\frac{\partial P}{\partial q_4} = \begin{bmatrix} 0 & 2q_5 & 2q_6 \\ 2q_5 & -4q_4 & -2q_7 \\ 2q_6 & 2q_7 & -4q_4 \end{bmatrix},$$

$$\frac{\partial P}{\partial q_5} = \begin{bmatrix} -4q_5 & 2q_4 & 2q_7 \\ 2q_4 & 0 & 2q_5 \\ -2q_7 & 2q_6 & -4q_5 \end{bmatrix},$$

$$\frac{\partial P}{\partial q_6} = \begin{bmatrix} -4q_6 & -2q_7 & 2q_4 \\ 2q_7 & -4q_6 & 2q_5 \\ 2q_4 & 2q_5 & 0 \end{bmatrix},$$

$$\frac{\partial P}{\partial q_7} = \begin{bmatrix} 0 & -2q_6 & 2q_5 \\ 2q_6 & 0 & -2q_4 \\ -2q_5 & 2q_4 & 0 \end{bmatrix}. \tag{50}$$

Finally,

$$\frac{\partial Q^\top}{\partial \sigma} = \begin{bmatrix} -\sin\sigma & -\cos\sigma & 0 \\ \cos\sigma & -\sin\sigma & 0 \\ 0 & 0 & 0 \end{bmatrix}. \tag{51}$$

4. J2 perturbation

When studying the J2 perturbation, the use of the Dromo formulation allows to obtain an analytical solution for the main problem as presented by Herrera-Montojo et al. [14] . However, in the presence of additional perturbing accelerations the applicability of an analytical solution is restricted. Here we present expressions to numerically obtain the STM which contains the J2 influence. The equations describing the J2 perturbing acceleration can be further simplified from Ref. 14) as we show in the following.

The J2 perturbing acceleration can be written in the $\mathcal{R}$ frame as

$$f_{J_2} = \frac{\alpha_2}{r^4} \begin{pmatrix} k_{rs2} \sin(2\sigma) + k_{rc2} \cos(2\sigma) + k_{r0} \\ k_{\theta s2} \sin(2\sigma) + k_{\theta c2} \cos(2\sigma) \\ k_{hs} \sin(\sigma) + k_{hc} \cos(\sigma) \end{pmatrix} \tag{52}$$

with $\alpha_2 = \mu J_2 R_E^2$, being $J_2 \simeq -1.08 \times 10^{-3}$ and R_E the Earth radius. The coefficients are given by

$$k_{r0} = -\frac{3}{2} + 9\left(q_4^2 + q_5^2\right)\left(q_6^2 + q_7^2\right) \tag{53a}$$

$$k_{rs2} = 18q_4 q_5 \left(q_6^2 - q_7^2\right) + 18q_6 q_7 \left(q_4^2 - q_5^2\right) \tag{53b}$$

$$k_{rc2} = 9\left(q_4^2 + q_5^2\right)\left(q_6^2 + q_7^2\right) - 18\left(q_4 q_7 + q_5 q_6\right)^2 \tag{53c}$$

$$k_{\theta s2} = 6\left(q_4^2 + q_5^2\right)\left(q_6^2 + q_7^2\right) - 12\left(q_4 q_7 + q_5 q_6\right)^2 \tag{53d}$$

$$k_{\theta c2} = -12q_4 q_5 \left(q_6^2 - q_7^2\right) - 12q_6 q_7 \left(q_4^2 - q_5^2\right) \tag{53e}$$

$$k_{hs} = -6\left(q_4 q_7 + q_5 q_6\right)\left(1 - 2q_4^2 - 2q_5^2\right) \tag{53f}$$

$$k_{hc} = -6\left(q_4 q_6 - q_5 q_7\right)\left(1 - 2q_4^2 - 2q_5^2\right) \tag{53g}$$

The gradient of the J2 perturbing acceleration can be expressed as

$$\frac{\partial f_{J_2}}{\partial q} = \begin{bmatrix} 4\frac{\cos\sigma}{s} f_{J_2} & 4\frac{\sin\sigma}{s} f_{J_2} & 4\frac{q_3+s}{q_3 s} f_{J_2} & \frac{\partial f_{J_2}}{\partial q_4} \cdots \frac{\partial f_{J_2}}{\partial q_7} & \frac{\partial f_{J_2}}{\partial \sigma} \end{bmatrix} \tag{54}$$

where for $i = 4, \cdots, 7$ we set

$$\frac{\partial f_{J_2}}{\partial q_i} = \frac{\alpha_2}{r^4} \begin{pmatrix} \frac{\partial k_{rs2}}{\partial q_i} \sin(2\sigma) + \frac{\partial k_{rc2}}{\partial q_i} \cos(2\sigma) + \frac{\partial k_{r0}}{\partial q_i} \\ \frac{\partial k_{\theta s2}}{\partial q_i} \sin(2\sigma) + \frac{\partial k_{\theta c2}}{\partial q_i} \cos(2\sigma) \\ \frac{\partial k_{hs}}{\partial q_i} \sin(\sigma) + \frac{\partial k_{hc}}{\partial q_i} \cos(\sigma) \end{pmatrix} \tag{55}$$

and

$$\frac{\partial f}{\partial \sigma} = -4\frac{u}{s} f_{J_2} + \frac{\alpha_2}{r^4} \begin{pmatrix} 2k_{rs2} \cos(2\sigma) - 2k_{rc2} \sin(2\sigma) \\ 2k_{\theta s2} \sin(2\sigma) - 2k_{\theta c2} \sin(2\sigma) \\ k_{hs} \cos(\sigma) - k_{hc} \sin(\sigma) \end{pmatrix} \tag{56}$$

The derivatives of the coefficients of the J2 acceleration are given by

$$\frac{\partial k_{r0}}{\partial q_3} = 18q_4 \left(q_6^2 + q_7^2\right), \tag{57a}$$

$$\frac{\partial k_{r0}}{\partial q_5} = 18q_5 \left(q_6^2 + q_7^2\right), \tag{57b}$$

$$\frac{\partial k_{r0}}{\partial q_6} = 18q_6 \left(q_4^2 + q_5^2\right), \tag{57c}$$

$$\frac{\partial k_{r0}}{\partial q_7} = 18q_7 \left(q_4^2 + q_5^2\right), \tag{57d}$$

$$\frac{dk_{rs2}}{dq_4} = 18q_5 \left(q_6^2 - q_7^2\right) + 36q_4 q_6 q_7, \tag{58a}$$

$$\frac{dk_{rs2}}{dq_5} = 18q_4 \left(q_6^2 - q_7^2\right) - 36q_5 q_6 q_7, \tag{58b}$$

$$\frac{dk_{rs2}}{dq_6} = 18q_7 \left(q_4^2 - q_5^2\right) + 36q_4 q_5 q_6, \tag{58c}$$

$$\frac{dk_{rs2}}{dq_7} = 18q_6 \left(q_4^2 - q_5^2\right) - 36q_4 q_5 q_7, \tag{58d}$$

$$\frac{\partial k_{rc2}}{\partial q_4} = 18q_4\left(q_6^2 - q_7^2\right) - 36q_5q_6q_7, \quad (59a)$$

$$\frac{\partial k_{rc2}}{\partial q_5} = -18q_5\left(q_6^2 - q_7^2\right) - 36q_4q_6q_7, \quad (59b)$$

$$\frac{\partial k_{rc2}}{\partial q_6} = 18q_6\left(q_4^2 - q_5^2\right) - 36q_4q_5q_7, \quad (59c)$$

$$\frac{\partial k_{rc2}}{\partial q_7} = -18q_7\left(q_4^2 - q_5^2\right) - 36q_4q_5q_6, \quad (59d)$$

$$\frac{\partial k_{\theta s2}}{\partial q_4} = 12q_4\left(q_6^2 - q_7^2\right) - 24q_5q_6q_7, \quad (60a)$$

$$\frac{\partial k_{\theta s2}}{\partial q_5} = -12q_5\left(q_6^2 - q_7^2\right) - 24q_4q_6q_7, \quad (60b)$$

$$\frac{\partial k_{\theta s2}}{\partial q_6} = 12q_6\left(q_4^2 - q_5^2\right) - 24q_4q_5q_7, \quad (60c)$$

$$\frac{\partial k_{\theta s2}}{\partial q_7} = -12q_7\left(q_4^2 - q_5^2\right) - 24q_4q_5q_6, \quad (60d)$$

$$\frac{\partial k_{\theta c2}}{\partial q_4} = -12q_5\left(q_6^2 - q_7^2\right) - 24q_4q_6q_7, \quad (61a)$$

$$\frac{\partial k_{\theta c2}}{\partial q_5} = -12q_4\left(q_6^2 - q_7^2\right) + 24q_5q_6q_7, \quad (61b)$$

$$\frac{\partial k_{\theta c2}}{\partial q_6} = -12q_7\left(q_4^2 - q_5^2\right) - 24q_4q_5q_6, \quad (61c)$$

$$\frac{\partial k_{\theta c2}}{\partial q_7} = -12q_6\left(q_4^2 - q_5^2\right) + 24q_4q_5q_7, \quad (61d)$$

$$\frac{\partial k_{hs}}{\partial q_4} = -6q_7\left(1 - 2q_4^2 - 2q_5^2\right) + 24q_4\left(q_4q_7 + q_5q_6\right), \quad (62a)$$

$$\frac{\partial k_{hs}}{\partial q_5} = -6q_6\left(1 - 2q_4^2 - 2q_5^2\right) + 24q_5\left(q_4q_7 + q_5q_6\right), \quad (62b)$$

$$\frac{\partial k_{hs}}{\partial q_6} = -6q_5\left(1 - 2q_4^2 - 2q_5^2\right), \quad (62c)$$

$$\frac{\partial k_{hs}}{\partial q_7} = -6q_4\left(1 - 2q_4^2 - 2q_5^2\right), \quad (62d)$$

$$\frac{\partial k_{hc}}{\partial q_4} = -6q_6\left(1 - 2q_4^2 - 2q_5^2\right) + 24q_4\left(q_4q_6 - q_5q_7\right), \quad (63a)$$

$$\frac{\partial k_{hc}}{\partial q_5} = 6q_7\left(1 - 2q_4^2 - 2q_5^2\right) + 24q_5\left(q_4q_6 - q_5q_7\right), \quad (63b)$$

$$\frac{\partial k_{hc}}{\partial q_6} = -6q_4\left(1 - 2q_4^2 - 2q_5^2\right), \quad (63c)$$

$$\frac{\partial k_{hc}}{\partial q_7} = 6q_5\left(1 - 2q_4^2 - 2q_5^2\right). \quad (63d)$$

5. Application and discussion

In order to assess the range of validity of the linear propagation using Dromo elements, a comparison with a fully numerical Monte-Carlo method is presented in this section. To this end, n_{MC} samples from the initial covariance matrix are drawn and propagated in time with both methods. A STM Cartesian coordinates based method was also included in this comparison

A set of highly-inclined orbits with varying eccentricity are chosen. The initial orbital elements are given in Table 1. The eccentricity is selected in the range 0.01–0.2. The initial uncertainty is assumed to follow an isotropic Gaussian distribution whose standard deviations for position and velocity are $\sigma_{\text{pos}} = 100\,\text{m}$ and $\sigma_{\text{vel}} = 1\,\text{mm\,s}^{-1}$.

Table 1. Initial conditions

a [km]	e	i [deg]	Ω [deg]	ω [deg]	ν [deg]
15000	0.01–0.2	80	30	-20	0

The dynamical model includes the gravitational influence of the Earth, Sun and Moon, and the $J2$ term of the geopotential model. The position of the perturbing bodies was obtained using the JPL ephemeris DE430, the initial epoch was set to 2017 January 1, and the uncertainty was propagated for seven days. For Earth orbits that do not approach the vicinity of the Moon, the effect of the perturbations on the uncertainty evolution is not significant. No significant difference on accuracy was found in numerical simulations when the perturbing effects were turned on or off. However the effect of perturbation does change the nominal orbit.

Two reasons lay behind: on the first place the STM is affected by the *gradient* of the perturbations, which is usually small (and the perturbation is usually small to begin with). Their effect can only be seen in long-term propagations, where the use of a linearized method may not be justified. Additionally, inspection of Eq. (33) makes it obvious that the Dromo elements evolution is proportional to the perturbing force, while the derivative of the fictitious-time σ only depends on the Dromo elements as previously stated. In the particular case of a circular orbit, the right hand side of Eq. (33h) becomes constant and the linearization error vanishes for σ. For increasing eccentricity, it becomes more important as the radial velocity u becomes not-zero and appears in the Hessian of the equations of motion. This has a direct impact on the linearization error.

The σ linearization error is present both on the Dromo-based method and its Cartesian coordinates based counterpart. It will affect more strongly those orbits which deviate more from the nominal trajectory. However when constructing a STM using Cartesian coordinates, a further approximation to the reality is introduced: even for circular orbits, errors on the tangential direction are projected onto the orbit tangent, instead of being contained on the orbit. The larger the angular uncertainty becomes, the more this error is observed.

Figure 2 shows the average error for a linear propagation using the Dromo and the Cartesian methods, in the case that the eccentricity takes small values ($e = 0.01$). The average error is defined as the position difference between the fully-numerical simulation and the linear approximations, averaged over the n_{MC} samples. The points with smaller initial error are likely

to show larger final errors that the points with higher initial deviations, but the latter are statistically less probable. Then, the average error can give a measure to compare both methods. For small eccentricities, the Dromo method greatly outperforms the Cartesian coordinates based method as the error is 1 to 2 orders of magnitude smaller.

For increasing values of the eccentricity, the Dromo method still shows advantages, as can be seen in Fig. 3 ($e = 0.1$) and Fig. 4 ($e = 0.2$). For very large values of eccentricity the linearization error for the Dromo method increases, but it always remain well below the error of the Cartesian coordinates method.
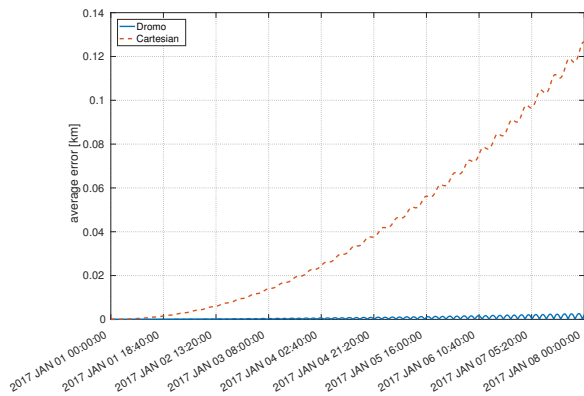
Fig. 2.   Average error for $e = 0.01$.
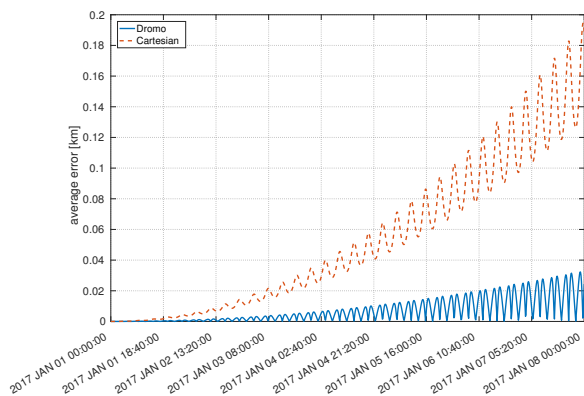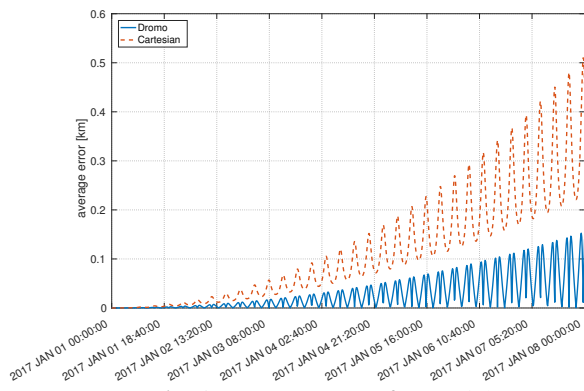

Fig. 3.   Average error for $e = 0.1$.

Fig. 4.   Average error for $e = 0.2$.

6.   Conclusion

In this paper a linear uncertainty propagation method was presented. The method hinges on the special perturbation method Dromo, which makes possible to obtain analytical, compact expressions of the necessary gradient matrices. Analysis of the equations reveals that the effect of the perturbations is small in the general case, and the accuracy of the algorithm depends on the linearization error of the Dromo fictitious-time.

The method was applied to study the evolution of the uncertainty of a satellite orbiting around an oblate planet in the presence of external body perturbations. The results were compared to Monte-Carlo simulations and a Cartesian coordinates linear method.

For small values of the eccentricity, the proposed method shows one to two orders of magnitude of improvement on the average error when propagating the uncertainty of Earth-bound orbits. For increasing values of the eccentricity the linearization error makes the results less accurate, but better in any case that when compared to Cartesian coordinates linear methods.

References

1) Junkins, J. L., Akella, M. R. and Alfriend, K. T.: Non-Gaussian error propagation in orbital mechanics, *The Journal of the Astronautical Sciences*, **44(4)** (1996), pp. 541–563.

2) Hernando-Ayuso, J. and Bombardelli, C.: Covariance Propagation Via Quadratic-Order State Transition Matrix in Curvilinear Coordinates, *Celestial Mechanics and Dynamical Astronomy*, submitted (Jan 2017).

3) Park, R. S. and Scheeres, D. J.: Nonlinear mapping of Gaussian statistics: theory and applications to spacecraft trajectory design, *Journal of guidance, Control, and Dynamics*, **29(6)** (2006), pp. 1367–1375.

4) Fujimoto, K. and Scheeres, D. J.: Tractable Expressions for Nonlinearly Propagated Uncertainties, *Journal of Guidance, Control, and Dynamics*, **38(6)** (2015. doi: 10.2514/1.G000795), pp. 1146–1151.

5) Peláez, J., Hedo, J. M. and de Andrés, P. R.: A special perturbation method in orbital dynamics, *Celestial Mechanics and Dynamical Astronomy*, **97(2)** (2007), pp. 131–150. doi: 10.1007/s10569–006–9056–3, dx.doi.org/10.1007/s10569-006-9056-3.

6) Urrutxua, H., Sanjurjo-Rivo, M. and Peláez, J.: DROMO propagator revisited, *Celestial Mechanics and Dynamical Astronomy*, **124(1)** (2015. doi: 10.1007/s10569-015-9647-y), pp. 1–31.

7) Baù, G., Bombardelli, C. and Peláez, J.: A new set of integrals of motion to propagate the perturbed two-body problem, *Celestial Mechanics and Dynamical Astronomy*, **116(1)** (2013. doi: 10.1007/s10569-013-9475-x), pp. 53–78.

8) Baú, G. and Bombardelli, C.: Time Elements for Enhanced Performance of the Dromo Orbit Propagator, *The Astronomical Journal*, **148(3)** (2014), p. 43.

9) Baú, G., Bombardelli, C., Pelez, J. and Lorenzini, E.: Non-singular orbital elements for special perturbations in the two-body problem, *Monthly Notices of the Royal Astronomical Society*, **454(3)** (2015), pp. 2890–2908.

10) Hernando-Ayuso, J. and Bombardelli, C.: Orbit Uncertainty Propagation Using Dromo, *AIAA/AAS Astrodynamics Specialist Conference*, AIAA 2016-5632, 2016.

11) Battin, R.: *An introduction to the mathematics and methods of astrodynamics*, AIAA, 1999.

12) Folkner, W. M., Williams, J. G., Boggs, D. H., Park, R. S. and Kuchynka, P.: The planetary and lunar ephemerides DE430 and DE431, *Interplanetary Network Progress Report 42-196*, **196** (2014), pp. 1–81.

13) Simon, J.-L., Francou, G., Fienga, A. and Manche, H.: New analytical planetary theories VSOP2013 and TOP2013, *Astronomy & Astrophysics*, **557** (2013), p. A49.

14) Herrera-Montojo, J., Urrutxua, H. and Peláez, J.: An asymptotic solution for the main problem., *AIAA/AAS Astrodynamics Specialist Conference*, AIAA 2014-4155, AIAA, San Diego, CA, 2014.